

# Channel Estimation for Ambient Backscatter Communication Systems with Massive-Antenna Reader

Wenjing Zhao, Gongpu Wang, Saman Atapattu, Ruisi He, and Ying-Chang Liang

arXiv:1904.03458v1 [eess.SP] 6 Apr 2019

**Abstract**—Ambient backscatter, an emerging green communication technology, has aroused great interest from both academia and industry. One open problem for ambient backscatter communication (AmBC) systems is channel estimation for a massive-antenna reader. In this paper, we focus on channel estimation problem in AmBC systems with uniform linear array (ULA) at the reader which consists of large number of antennas. We first design a two-step method to jointly estimate channel gains and direction of arrivals (DoAs), and then refine the estimates through angular rotation. Additionally, Cramér-Rao lower bounds (CRLBs) are derived for both the modulus of the channel gain and the DoA estimates. Simulations are then provided to validate the analysis, and to show the efficiency of the proposed approach.

**Index Terms**—Ambient backscatter, channel estimation, direction of arrivals (DoAs), discrete Fourier transformation (DFT)

## I. INTRODUCTION

Aiming to enable easy access and interaction among numerous computing devices such as sensors or tags, Internet of Things (IoT) will play a vital role in the future communication paradigm [1], [2]. Recently, there has been many work on different research directions on IoT. Among them, how sustained and reliable energy can be supplied to large-scale deployments of IoT devices is an interesting and challenging problem nowadays. Since ambient backscatter leverages environmental radio frequency (RF) signals to enable battery-free devices to communicate with each other, it has high potential to offer a solution for the energy problem in IoT systems [3]. An ambient backscatter communication (AmBC) system typically consists of a RF source, a reader and a tag. Before modulating its own binary data, the tag first harvests energy from RF signals, which thus exempts the tag from energy constraint. Then, the tag loads bit ‘1’ by reflecting the incident RF signals and bit ‘0’ by absorbing them. By using certain detector, such as maximum-likelihood (ML) detector, the reader demodulates the bit information accordingly [4].

W. Zhao and G. Wang are with Beijing Key Lab of Transportation Data Analysis and Mining, School of Computer and Information Technology, Beijing Jiaotong University, China (e-mail: {wenjingzhao, gpwang}@bjtu.edu.cn). S. Atapattu is with the Department of Electrical and Electronic Engineering, University of Melbourne, Parkville, VIC 3010, Australia (e-mail: saman.atapattu@unimelb.edu.au). R. He is with the State Key Laboratory of Rail Traffic Control and Safety, Beijing Jiaotong University, China (e-mail: ruisi.he@bjtu.edu.cn). Y.-C. Liang is with the Center for Intelligent Networking and Communications, University of Electronic Science and Technology of China, Chengdu 611731, China (e-mail: liangyc@ieee.org).

The majority of existing theoretical studies on AmBC, related to signal detection [4], [5] and the references therein, performance analysis [6], [7] and multiple access scheme [8], assume perfect channel state information (CSI). In reality, precise knowledge of full CSI is not always possible, especially with strict energy constrained IoT systems. As the tag may not be able to transmit pilots, traditional methods of channel estimation may not be directly applied to AmBC systems. The inconsistencies of channels at reflective and absorptive states also pose a great challenge on channel estimation. Taking these into account, an expectation maximization (EM) based estimator is designed to acquire the modulus values of channels in an AmBC system with a single-antenna reader in [9]. In a multiple-antenna reader circumstance, an approach on the strength of eigenvalue decomposition (EVD) [10] is adopted to retrieve channel parameters. Nevertheless, the complexity of EVD is prohibitive in AmBC systems with massive-antenna reader, which motivates our work. In this paper, we tackle the channel estimation problem in AmBC systems with massive-antenna reader having an uniform linear array (ULA). Together with least-square (LS) method, an estimator resorting to discrete Fourier transformation (DFT) [11] and angular rotation operation is presented to collectively figure out the direction of arrivals (DoAs) and channel gains.

**Notations:** We use boldfaced lowercase for vectors and boldface uppercase for matrices. The transpose and the inverse of matrix  $\mathbf{X}$  are denoted by  $\mathbf{X}^T$  and  $\mathbf{X}^{-1}$ , respectively.  $[\mathbf{X}]_{ij}$  indicates the  $(i, j)$ th element of matrix  $\mathbf{X}$ , and  $\mathbf{x}_i$  indicates the  $i$ th element of vector  $\mathbf{x}$ .  $\text{diag}\{\mathbf{x}\}$  denotes a square diagonal matrix with the elements of  $\mathbf{x}$  on the main diagonal. The identity matrix is denoted by  $\mathbf{I}$ .  $\mathbf{x} \sim \mathcal{CN}(\mu, \Sigma)$  denotes that  $\mathbf{x}$  is a circularly symmetric complex Gaussian (CSCG) vector with mean  $\mu$  and covariance matrix  $\Sigma$ .  $\|\mathbf{x}\|$  represents the 2-norm of vector  $\mathbf{x}$ .  $\lfloor x \rfloor$  rounds  $x$  to the nearest integer, and  $\mathbb{E}\{x\}$  means the statistical expectation of  $x$ .

## II. SYSTEM MODEL

As shown in Fig. 1, we consider an AmBC system with a RF source ( $S$ ), a reader ( $R$ ) equipped with  $M$  antennas in the form of ULA, and a passive tag ( $T$ ) with single antenna. The reader not only receives signal from the RF source directly, but also collects signal backscattered from the tag. The tag first harvests energy from the RF signals. By intentionally changing its load impedance, the tag then piggybacks its information bits over ambient RF carriers to backscatter outside or to absorb inside the received signals.

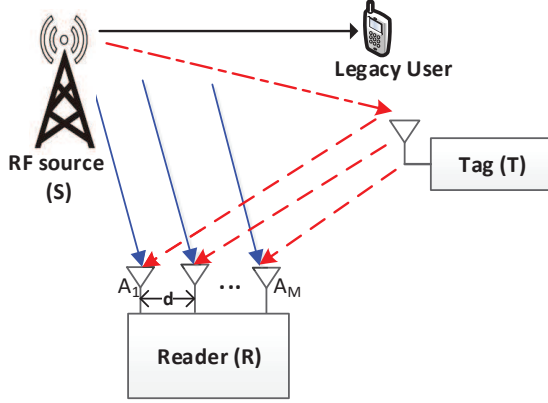


Fig. 1. An ambient backscatter communication (AmBC) system with a massive-antenna reader.

Let  $s(n)$  be the signals from the RF source with power  $P_s$  and  $B(n) \in \{0, 1\}$  the modulated signal at the tag which keeps unchanged during  $N$  consecutive RF signals. Define  $\theta_0 \in [-\frac{\pi}{2}, \frac{\pi}{2}]$  and  $\theta_1 \in [-\frac{\pi}{2}, \frac{\pi}{2}]$  as the signal azimuth angles or DoAs of paths  $S - R$  and  $T - R$ , respectively. Denote channel gains of  $S - R$ ,  $S - T$  and  $T - R$  as  $h_0$ ,  $h_{st}$  and  $h_{tr}$ , respectively. The attenuation factor inside the tag is denoted as  $\eta \in (0, 1]$ . Then, the received signal at the reader is [12]

$$\begin{aligned} \mathbf{y}(n) &= \mathbf{h}_{sr}s(n) + \mathbf{h}_{tr}\eta h_{st}s(n)B(n) + \mathbf{w}(n) \\ &= \mathbf{h}\mathbf{s}(n) + \mathbf{w}(n), \end{aligned} \quad (1)$$

where  $\mathbf{h}_{sr} = h_0[1, e^{j\frac{2\pi d}{\lambda} \sin \theta_0}, \dots, e^{j\frac{2\pi d}{\lambda} (M-1) \sin \theta_0}]^T$ ,  $\mathbf{h}_{tr} = h_{tr}[1, e^{j\frac{2\pi d}{\lambda} \sin \theta_1}, \dots, e^{j\frac{2\pi d}{\lambda} (M-1) \sin \theta_1}]^T$ ,  $\mathbf{h} = \mathbf{h}_{sr} + \eta h_{st} \mathbf{h}_{tr} B(n)$  and  $\mathbf{w}(n)$  is CSCG noise vector distributed as  $\mathbf{w}(n) \sim \mathcal{CN}(\mathbf{0}, \sigma^2 \mathbf{I})$ . Here,  $d$  is the distance between two adjacent antennas and  $\lambda$  is the wave length of the RF signal.

### III. DOAS AND CHANNEL GAINS ESTIMATION

This section describes the procedure for the estimation of the DoAs and the channel gains. The technique is divided into the following three steps: i) the channel  $\mathbf{h}$  in the absorptive or reflective state is incipiently retrieved by means of LS; ii) by performing DFT operation on the channel  $\mathbf{h}$ , coarse DoAs  $[\theta_0, \theta_1]$  and gains  $[h_0, \frac{h_1}{\eta}]$  can be obtained; and iii) with the aid of angular rotation, fine estimates of both the DoAs and the channel gains are acquired.

#### Step 1: Initial Channel Estimation

Prior to the tag modulates its own data, while the tag initially transmits  $2N$  control sequences, the RF source transmits  $2N$  pilots. Specifically, the tag transmits bit '0' during the first  $N$  RF symbols and bit '1' during the following  $N$  RF symbols. For  $B(n) = i, i \in \{0, 1\}$ , we denote  $N$  RF pilots as  $\mathbf{s} = [s_1, s_2, \dots, s_N]^T$  and each element has modulus  $\sqrt{P_s}$ , i.e.,  $|\mathbf{s}_n|^2 = P_s$ . Then, the received signal matrix of size  $M \times N$  at the reader is

$$\mathbf{Y} = \mathbf{h}\mathbf{s}^T + \mathbf{W}, \quad (2)$$

where  $\mathbf{W}$  is the  $M \times N$  noise matrix. Then, an LS estimator for the desired channel  $\mathbf{h}$  is

$$\hat{\mathbf{h}}^{\text{LS}} = \mathbf{Y}\mathbf{s}(\mathbf{s}^T\mathbf{s})^{-1} = \mathbf{h} + \frac{\mathbf{W}\mathbf{s}}{NP_s}. \quad (3)$$

#### Step 2: Coarse DoAs and Gains Estimation via DFT

We define the DFT matrix as

$$[\mathbf{F}]_{pq} = \frac{1}{M} e^{-j\frac{2\pi}{M}(p-1)(q-1)}, \quad p, q \in \{1, \dots, M\}. \quad (4)$$

Then, the DFT of the channel  $\mathbf{h}$  is

$$\hat{\mathbf{h}}^{\text{DFT}} = \mathbf{F}\mathbf{h}, \quad (5)$$

whose  $m$ th entry can be calculated as

$$\begin{aligned} \hat{\mathbf{h}}_m^{\text{DFT}} &= \frac{h_0}{M} e^{-j\frac{M-1}{2}r_0} \frac{\sin(\frac{M}{2}r_0)}{\sin(\frac{1}{2}r_0)} \\ &+ \frac{h_1 B(n)}{M} e^{-j\frac{M-1}{2}r_1} \frac{\sin(\frac{M}{2}r_1)}{\sin(\frac{1}{2}r_1)}, \end{aligned} \quad (6)$$

where  $r_i = \frac{2\pi(m-1)}{M} - \frac{2\pi d}{\lambda} \sin \theta_i$  for  $i \in \{0, 1\}$ , and  $h_1 = \eta h_{st} h_{tr}$ . According to (6), if  $\frac{Md}{\lambda} \sin \theta_i + 1$  is equal to certain integer  $m$ ,  $\hat{\mathbf{h}}^{\text{DFT}}$  has only one non-zero item  $\hat{\mathbf{h}}_m^{\text{DFT}} = h_i$  when  $M \rightarrow \infty$ . This means that the channel power is centred on only one position  $m = \frac{Md}{\lambda} \sin \theta_i + 1$ . Further, the DoAs and the channel gains can be separately estimated as

$$\hat{\theta}_i^{\text{DFT}} = \begin{cases} \arcsin\left(\frac{(m-1-M)\lambda}{Md}\right), & \theta_i \in [-\frac{\pi}{2}, 0] \\ \arcsin\left(\frac{(m-1)\lambda}{Md}\right), & \theta_i \in [0, \frac{\pi}{2}] \end{cases} \quad (7)$$

$$\hat{h}_i^{\text{DFT}} = \hat{\mathbf{h}}_m^{\text{DFT}}. \quad (8)$$

However, the actual situation is that  $\frac{Md}{\lambda} \sin \theta_i$  is not always an integer, where we can take  $m = \lfloor \frac{Md}{\lambda} \sin \theta_0 \rfloor + 1$ .

#### Step 3: Refining Estimates Through Angular Rotation

Performing angular rotation operation yields

$$\hat{\mathbf{h}}^{\text{Ro}} = \mathbf{F}\Phi(\Delta_i)\mathbf{h}, \quad (9)$$

where  $\Phi(\Delta_i) = \text{diag}\{1, e^{j\Delta_i}, \dots, e^{j(M-1)\Delta_i}\}$  is angular rotation matrix for  $\Delta_i \in [-\frac{\pi}{M}, \frac{\pi}{M}]$ . Similarly, the  $m$ th element of  $\hat{\mathbf{h}}^{\text{Ro}}$  has the form as

$$\begin{aligned} \hat{\mathbf{h}}_m^{\text{Ro}} &= \frac{h_0}{\sqrt{M}} e^{-j\frac{M-1}{2}\tilde{r}_0} \frac{\sin(\frac{M}{2}\tilde{r}_0)}{\sin(\frac{1}{2}\tilde{r}_0)} \\ &+ \frac{h_1 B(n)}{\sqrt{M}} e^{-j\frac{M-1}{2}\tilde{r}_1} \frac{\sin(\frac{M}{2}\tilde{r}_1)}{\sin(\frac{1}{2}\tilde{r}_1)}, \end{aligned} \quad (10)$$

where  $\tilde{r}_i = \frac{2\pi(m-1)}{M} - \frac{2\pi d}{\lambda} \sin \theta_i - \Delta_i$  for  $i \in \{0, 1\}$ . Obviously, there always exists  $\Delta_i$  which makes

$$m = \frac{Md}{\lambda} \sin \theta_i + \frac{M\Delta_i}{2\pi} + 1, \quad (11)$$

an integer. Then, we can refine the corresponding parameters as

$$\hat{\theta}_i^{\text{Ro}} = \begin{cases} \arcsin\left(\frac{(m-1-M)\lambda}{Md} - \frac{\Delta_i\lambda}{2\pi d}\right), & \theta_i \in [-\frac{\pi}{2}, 0] \\ \arcsin\left(\frac{(m-1)\lambda}{Md} - \frac{\Delta_i\lambda}{2\pi d}\right), & \theta_i \in [0, \frac{\pi}{2}] \end{cases} \quad (12)$$

$$\hat{h}_i^{\text{Ro}} = \hat{\mathbf{h}}_m^{\text{Ro}}. \quad (13)$$

*Remark 1:* The presented method is also applicable to channel estimation in multi-path or frequency-selective channels scenarios since the composite channel in the case of  $B(n) = 1$  can be treated as a combination of paths  $S - R$  and  $S - T - R$ .

#### IV. CRAMÉR-RAO LOWER BOUNDS

In this section, we compute the CRLBs for the modulus of the channel gain and the DoA estimates. Suppose  $h_0 = |h_0|e^{j\omega_0}$  and  $h_1 = |h_1|e^{j\omega_1}$ . Let us define vector  $\varphi = [|h_0|, |h_1|, \sin \theta_0, \sin \theta_1]^T$  and  $g(\varphi) = [|h_0|, \frac{|h_1|}{\eta}, \theta_0, \theta_1]^T$ . For a given  $\varphi$ , the probability density function  $p(\mathbf{y}; \varphi)$  of  $\mathbf{y} = [\mathbf{y}^T(N+1), \dots, \mathbf{y}^T(2N)]^T$  during  $N$  consecutive RF signals is

$$p(\mathbf{y}; \varphi) = \frac{\pi^{-MN}}{\sigma^{2MN}} \prod_{n=N+1}^{2N} e^{-\frac{\|\mathbf{y}(n) - (\mathbf{h}_{sr} + \eta \mathbf{h}_{st} \mathbf{h}_{tr})s(n)\|^2}{\sigma^2}}. \quad (14)$$

The Fisher information matrix of vector  $\varphi$  is defined as [13]

$$[\mathbf{I}(\varphi)]_{m,n} = -\mathbb{E} \left\{ \frac{\partial^2 \ln p(\mathbf{y}; \varphi)}{\partial \varphi_m \partial \varphi_n} \right\}. \quad (15)$$

Let  $c_0 = \frac{2\pi d}{\lambda}$ ,  $c_1 = \frac{2\pi d}{\lambda}(\sin \theta_0 - \sin \theta_1)$  and  $c_2 = \omega_0 - \omega_1$ , and the Fisher information matrix and its entries are

$$\mathbf{I}(\varphi) = \frac{2NP_s}{\sigma^2} \begin{pmatrix} T_{11} & T_{12} & 0 & T_{14} \\ T_{12} & T_{22} & T_{23} & 0 \\ 0 & T_{23} & T_{33} & T_{34} \\ T_{14} & 0 & T_{34} & T_{44} \end{pmatrix} \quad (16)$$

$$\begin{aligned} T_{11} &= M, \quad T_{12} = \sum_{m=0}^{M-1} \cos(c_1 m + c_2), \\ T_{14} &= c_0 |h_1| \sum_{m=0}^{M-1} m \sin(c_1 m + c_2), \quad T_{22} = M, \\ T_{23} &= -c_0 |h_0| \sum_{m=0}^{M-1} m \sin(c_1 m + c_2), \\ T_{33} &= \frac{c_0^2 h_0^2 (M-1) M (2M-1)}{3}, \\ T_{34} &= c_0^2 |h_0 h_1| \sum_{m=0}^{M-1} m^2 \cos(c_1 m + c_2), \\ T_{44} &= \frac{c_0^2 h_1^2 (M-1) M (2M-1)}{3}. \end{aligned}$$

Afterwards, the CRLBs of  $g(\varphi)$  can be derived by using the inequality:

$$\begin{aligned} \text{var}([\hat{g}(\varphi)]_{m,1}) &\geq \left[ \frac{\partial g(\varphi)}{\partial \varphi} \mathbf{I}^{-1}(\varphi) \frac{\partial g(\varphi)}{\partial \varphi}^T \right]_{mm} \\ &= \left[ \frac{\partial g(\varphi)}{\partial \varphi} \right]_{mm}^2 [\mathbf{I}^{-1}(\varphi)]_{mm}, \end{aligned} \quad (17)$$

where  $\frac{\partial g(\varphi)}{\partial \varphi} = \text{diag} \left\{ 1, \frac{1}{\eta}, \frac{1}{\cos \theta_0}, \frac{1}{\cos \theta_1} \right\}$ .

Based on (16) and (17), the CRLBs of the modulus of the channel gains and the DoAs in the case of  $B(n) = 1$  can be

respectively formulated as

$$\begin{aligned} \text{var}(|\hat{h}_0|) &\geq \frac{\sigma^2 (T_{22} T_{33} T_{44} - T_{22} T_{34}^2 - T_{23}^2 T_{44})}{2N L_1 P_s}, \\ \text{var}\left(\frac{|\hat{h}_1|}{\eta}\right) &\geq \frac{\sigma^2 (T_{11} T_{33} T_{44} - T_{14}^2 T_{33} - T_{11} T_{34}^2)}{2N L_1 P_s \eta^2}, \\ \text{var}(\hat{\theta}_0) &\geq \frac{\sigma^2 (T_{11} T_{22} T_{44} - T_{22} T_{14}^2 - T_{12}^2 T_{44})}{2N L_1 P_s \cos^2 \theta_0}, \\ \text{var}(\hat{\theta}_1) &\geq \frac{\sigma^2 (T_{11} T_{22} T_{33} - T_{11} T_{23}^2 - T_{12}^2 T_{33})}{2N L_1 P_s \cos^2 \theta_1}, \end{aligned} \quad (18)$$

where

$$\begin{aligned} L_1 = & \left( T_{14}^2 (T_{23}^2 - T_{22} T_{33}) - 2T_{12} T_{14} T_{23} T_{34} \right. \\ & \left. + (T_{12}^2 - T_{11} T_{22}) (T_{34}^2 - T_{33} T_{44}) - T_{11} T_{23}^2 T_{44} \right). \end{aligned} \quad (19)$$

Considering that  $[\mathbf{I}^{-1}(\varphi)]_{mm} \geq [\mathbf{I}(\varphi)]_{mm}^{-1}$ , we obtain a lower bound of CRLBs (LCRLBs) in the case of  $B(n) = 1$  as

$$\text{var}([\hat{g}(\varphi)]_{m,1}) \geq \left[ \frac{\partial g(\varphi)}{\partial \varphi} \right]_{mm}^2 \frac{1}{[\mathbf{I}(\varphi)]_{mm}}. \quad (20)$$

Consequently, the corresponding LCRLBs can be shown as

$$\text{var}(|\hat{h}_0|) \geq \frac{\sigma^2}{2MNP_s}, \quad \text{var}\left(\frac{|\hat{h}_1|}{\eta}\right) \geq \frac{\sigma^2}{2MNP_s \eta^2}, \quad (21)$$

$$\text{var}(\hat{\theta}_0) \geq \frac{3\lambda^2 \sigma^2}{(2\pi d)^2 N(M-1)M(2M-1)h_0^2 P_s \cos^2 \theta_0}, \quad (22)$$

$$\text{var}(\hat{\theta}_1) \geq \frac{3\lambda^2 \sigma^2}{(2\pi d)^2 N(M-1)M(2M-1)h_1^2 P_s \cos^2 \theta_1}. \quad (23)$$

In a similar way, the CRLBs of the modulus of the channel gain and the DoA for  $B(n) = 0$  can be derived as  $\text{var}(|\hat{h}_0|)$  in (21) and (22), respectively.

*Remark 2:* As shown in Fig. 2 and Fig. 3, the related curves of the CRLBs and LCRLBs fit well. Accordingly, we can replace the CRLBs (18) with LCRLBs (21)-(23), which are more straightforward for performance analysis.

#### V. SIMULATION RESULTS

In this section, we select  $N = 1$ ,  $\sigma^2 = 1$  and  $\eta = 0.5$ . The reader is configured with  $M = 128$  antennas. The DoAs are set to  $\theta_0 = -\frac{\pi}{4}$  and  $\theta_1 = \frac{\pi}{5}$ . All fading channels are modeled as  $h_0, h_{st}, h_{tr} \sim \mathcal{CN}(0, 1)$ . Here, the mean square error (MSE) of an estimator  $\hat{x}$  is the average squared difference between the estimated result  $\hat{x}$  and what is estimated  $x$ , i.e.,  $\text{MSE}(\hat{x}) = \mathbb{E}\{(x - \hat{x})^2\}$ .

Fig. 2 displays MSEs of DoAs versus transmit SNR and Fig. 3 shows MSEs of the modulus of channel gains versus transmit SNR. According to our analysis in Section IV, the CRLBs of  $\theta_0$  and  $|h_0|$  in the case of  $B(n) = 0$  are equal to the corresponding LCRLBs in the case of  $B(n) = 1$ . Therefore, we omit the CRLB curves in the case of  $B(n) = 0$ . Both MSEs and CRLBs of the DoAs and the modulus of channel gains decrease with the increase of transmit SNR. It can be found that the corresponding CRLB curves are exactly below the corresponding MSE curves of our proposed estimator, which

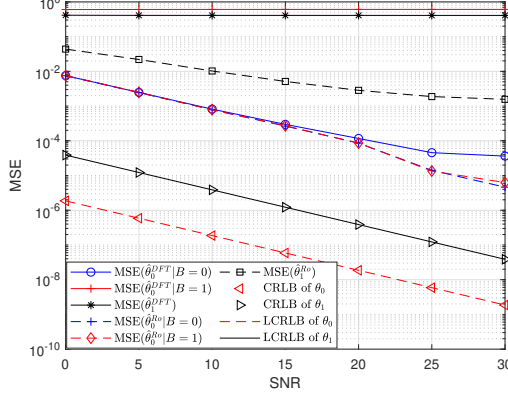


Fig. 2. MSE of DOA versus transmit SNR.

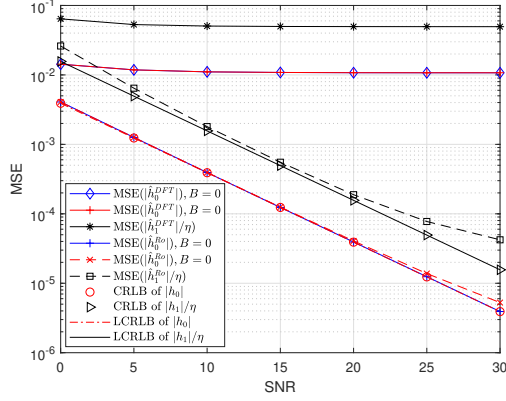


Fig. 3. MSE of channel gain versus transmit SNR.

verifies the validity of our theoretical derivations in (18). Fig. 4 depicts MSEs of estimates of  $\mathbf{h}$  versus transmit signal-to-noise ratio (SNR). As expected, the DFT-based estimator with angular rotation ('+' marked curves) performs better than that without rotation ('□' marked curves). We also observe that DFT-based estimator with angular rotation outperforms the traditional LS estimator (solid curves).

To show the impact of our proposed channel estimation on

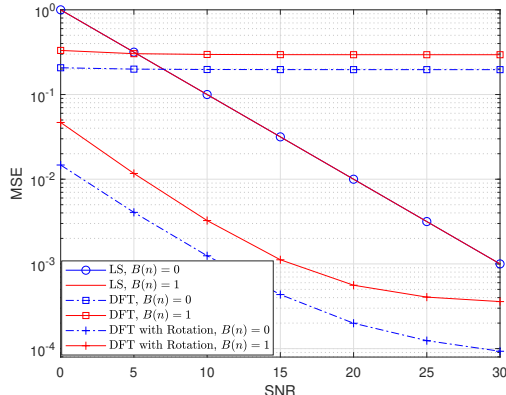


Fig. 4. MSE of channel versus transmit SNR.

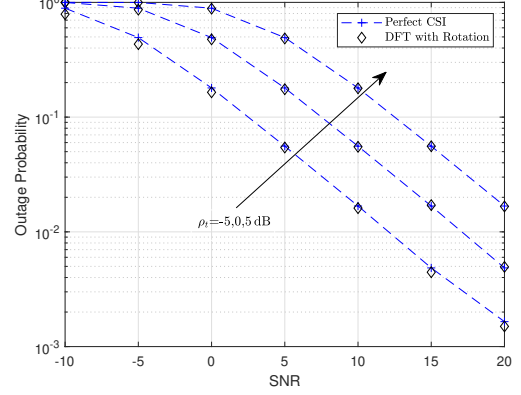


Fig. 5. Outage probability versus transmit SNR.

actual performance, Fig. 5 illustrates outage probability versus transmit SNR when threshold  $\rho_t$  is set to  $-5, 0, 5$  dB, where we use the selection combining reception at the reader. It can be seen that the gap between outage performance with perfect CSI assumption and that with channel estimated by our proposed method is negligible over the simulated range.

## VI. CONCLUSION

In this paper, we proposed a channel estimation technique for an ambient backscatter communication system with a massive-antenna reader. We tackled the channel estimation problem based on a signal processing standpoint as channels can be decomposed into channel gains and DoAs. First, preliminary channel estimates at different states were acquired by the LS estimation. Coupled with angular rotation, we then obtained both the channel gains and the DoAs by conducting DFT to the estimates. It is revealed that the proposed method separately featured high estimation accuracy and low complexity compared to the LS and EVD estimators.

## REFERENCES

- [1] Y. Zhou, H. Liu, Z. Pan, L. Tian, and J. Shi, "Spectral- and energy-efficient two-stage cooperative multicast for LTE-Advanced and beyond," *IEEE Wireless Commun. Mag.*, vol. 21, no. 2, pp. 34–41, Apr. 2014.
- [2] A. Al-Fuqaha, M. Guizani, M. Mohammadi, M. Aledhari, and M. Ayyash, "Internet of Things: A survey on enabling technologies, protocols, and applications," *IEEE Commun. Surveys Tuts.*, vol. 17, no. 4, pp. 2347–2376, Jun. 2015.
- [3] V. Liu, A. Parks, V. Talla, S. Gollakota, D. Wetherall, and J. R. Smith, "Ambient backscatter: wireless communication out of thin air," in *Proc. SIGCOMM*, Hong Kong, China, 2013, pp. 39–50.
- [4] Q. Tao, C. Zhong, K. Huang, X. Chen, and Z. Zhang, "Ambient backscatter communications systems with mfsk modulation," accepted by *IEEE Trans. Wireless Commun.*, 2019, doi: 10.1109/TWC.2019.2904964.
- [5] Q. Tao, C. Zhong, H. Lin, and Z. Zhang, "Symbol detection of ambient backscatter systems with Manchester coding," *IEEE Trans. Wireless Commun.*, vol. 17, no. 6, pp. 4028–4038, Jun. 2018.
- [6] W. Zhao, G. Wang, S. Atapattu, C. Tellambura, and H. Guan, "Outage analysis of ambient backscatter communication systems," *IEEE Commun. Lett.*, vol. 22, no. 8, pp. 1736–1739, Aug. 2018.
- [7] D. Li and Y. Liang, "Adaptive ambient backscatter communication systems with MRC," *IEEE Trans. Veh. Technol.*, vol. 67, no. 12, pp. 12 352–12 357, Dec. 2018.
- [8] W. Liu, Y. Liang, Y. Li, and B. Vucetic, "Backscatter multiplicative multiple-access systems: Fundamental limits and practical design," *IEEE Trans. Wireless Commun.*, vol. 17, no. 9, pp. 5713–5728, Sep. 2018.

- [9] S. Ma, G. Wang, R. Fan, and C. Tellambura, "Blind channel estimation for ambient backscatter communication systems," *IEEE Commun. Lett.*, vol. 22, no. 6, pp. 1296–1299, Jun. 2018.
- [10] W. Zhao, G. Wang, S. Atapattu, and B. Ai, "Blind channel estimation in ambient backscatter communication systems with multiple-antenna reader," in *IEEE/CIC Int. Conf. Commun. in China (ICCC)*, Aug. 2018, pp. 320–324.
- [11] D. Fan, F. Gao, G. Wang, Z. Zhong, and A. Nallanathan, "Angle domain signal processing-aided channel estimation for indoor 60-GHz TDD/FDD massive MIMO systems," *IEEE J. Select. Areas Commun.*, vol. 35, no. 9, pp. 1948–1961, Sep. 2017.
- [12] G. Wang, F. Gao, R. Fan, and C. Tellambura, "Ambient backscatter communication systems: Detection and performance analysis," *IEEE Trans. Commun.*, vol. 64, no. 11, pp. 4836–4846, Nov. 2016.
- [13] C. W. Helstrom, *Elements of signal detection and estimation*. Prentice-Hall, Inc., 1994.